

Alpha-Particle Irradiation of Ge at 4.2°K*

G. W. GOBELI

Department of Physics, Purdue University, Lafayette, Indiana

(Received July 14, 1958)

Degenerate *n*- and *p*-type germanium samples were irradiated at 4.2°K with polonium alpha-particles. The irradiation removed carriers at a rate of 2.84×10^4 electrons/ α -cm in *n*-type samples and 1.32×10^4 holes/ α -cm in *p*-type samples. Thermal recovery was studied up to 78°K. No measurable recovery was observed below 22°K. Upon warming to 78°K the irradiation-induced changes of Hall coefficient decreased by about the same fraction, 25% and 22%, respectively, in *n*-type and *p*-type samples, showing that the same fractions of donor and acceptor defects were annealed out. Experiments made with various annealing procedures, using electrical resistivity as a measure, indicated that there were two distinct regions of thermal recovery, with maximum rates of change occurring near 33°K and 67°K. The low-temperature process appears to follow a first-order reaction with a unique activation energy of about 0.02 ev. It may be due to the recombination of interstitials with nearby vacancies. The higher temperature process does not yield to simple analysis.

I. INTRODUCTION

THE general features of irradiation-produced changes in the electrical properties of germanium have been well established by experiments at Purdue¹ and Oak Ridge.² The results of these experiments led James and Lark-Horovitz³ to postulate a model for the energy level scheme of the defects introduced by irradiation. According to the model, the interstitial atoms of the Frenkel defects act as donors while the vacancies act as acceptors. The model allowed for deep-lying levels corresponding to multiple ionizations of the defects and indicated that only the first two ionizations of each type of defect fell within the energy gap.

The assumption is usually made that interstitials and vacancies are created in equal numbers by irradiation. In degenerate samples, all defect levels are either occupied (*n* type) or unoccupied (*p* type). Hence on the basis of the James-Lark-Horovitz model, carriers should be removed at the same rate in *n*-type and *p*-type samples. However, it has been observed experimentally that carrier removal rates, as determined from Hall coefficient and resistivity measurements, are significantly lower for *p*-type germanium than for *n* type. In the case of deuterium irradiations at 90°K, the observed carrier removal rates for *n*-type and *p*-type samples differ by a factor of about four.⁴

The possibility that this difference might be due to selective annealing of defects of one type indicates that experiments should be performed at the lowest possible temperatures. Low-temperature ($T \approx 15^\circ\text{K}$) irradiations and subsequent annealing experiments have been reported for copper, and silver,⁵ and recently for ger-

manium.⁶ In the metals, extensive annealing was observed near 40°K but in neutron-irradiated germanium the major effect reported was the disappearance of minority carrier traps at temperatures above 95°K.

The present report concerns irradiation of germanium samples at 4.2°K and the study of annealing up to 78°K. Polonium alpha-particles were used for the irradiation because the irradiation source simplified low-temperature instrumentation. A special method of preparing the samples was necessary in view of the short range of the alpha-particles in germanium.

II. EXPERIMENTAL PROCEDURES

The alpha-particle source used in these experiments consisted of a $\frac{1}{2}$ -in. diameter stainless-steel disk upon which 494 mC of $^{84}\text{Po}^{210}$ ($T_{1/2} = 138.4$ days, $E_\alpha = 5.30$ Mev) was deposited. The active area was covered with a thin stainless-steel window and the energy of alpha-particles incident on the sample was thereby reduced to 3.73 Mev. The alpha-particle flux was found by determining the absolute intensity of the source and multiplying by a geometrical factor which took into account the broad area of the source. This simple technique has been found to be in agreement with flux values determined by collection of the alpha-particle current.⁷

The very short range of alpha-particles in germanium (12.3 microns for alpha-particles of 3.73 Mev⁸) necessitated a special technique for the preparation of extremely thin samples. It has been shown⁹ that the electrical properties of such thin germanium layers prepared by etching and grinding from bulk material are the same as those of the parent material at all temperatures down to 1.3°K, provided extreme care is taken to avoid straining of the thin sample. Because

* Work supported in part by U. S. Signal Corps.

¹ H. Y. Fan and K. Lark-Horovitz, *Report of the Bristol Conference on Defects in Crystalline Solids, July, 1954* (Physical Society, London, 1955).

² Cleland, Crawford, Jr., Lark-Horovitz, Pigg, and Young, *Phys. Rev.* **83**, 861 (1951).

³ H. M. James and K. Lark-Horovitz, *Z. physik. Chem.* **198**, 107 (1951).

⁴ D. Kleitman, Ph.D. thesis, Purdue University, 1958 (unpublished).

⁵ Cooper, Koehler, and Marx, *Phys. Rev.* **97**, 599 (1955).

⁶ J. W. Cleland and J. H. Crawford, Jr., *J. Appl. Phys.* **29**, 151 (1958).

⁷ W. M. Becker, Ph.D. thesis, Purdue University, 1957 (unpublished).

⁸ G. W. Gobeli, *Phys. Rev.* **103**, 275 (1956).

⁹ C. M. Kellett, Jr., M. S. thesis, Purdue University, 1956 (unpublished).

of their extreme fragility, it was necessary to support the samples firmly on a substrate. The thermal expansion coefficient of this substrate had to be the same as that of the sample to avoid strain during temperature-cycling.

Special germanium flats for sample supports were prepared from impure *n*-type material. These substrates were irradiated until the resistance between surface points separated by 1 mm was greater than 10^7 ohms at 78°K. The electrical properties of germanium so treated are insensitive to the additional moderate fluxes received from the polonium source during the irradiation experiment.

All samples used in the irradiation studies were cut from germanium single-crystal ingots doped with antimony (*n* type) or gallium (*p* type). The samples were chosen to be extremely impure, with initial *n*-type Hall coefficient values of the order of -8 cm³/coul and initial *p*-type Hall coefficient values of the order of $+3$ cm³/coul, so that the Fermi level remained deep within the carrier band throughout the irradiation experiments.

The samples were carefully ground, polished, and etched in a hot (75°C) mixed acids bath and were firmly glued with Armstrong C-1 cement to the substrates previously described during the final preparation stages and throughout the experiments. The final thickness ranged from 3.5 to 8.0 microns. Electrical contacts were made by soldering No. 40 gauge copper wires directly to the sample.

The cryostat employed for the irradiations at liquid helium temperature is of the gas exchange type used by Fritzsche¹⁰ with a modification allowing mechanical motion of a shutter for controlling the progress of the irradiation. The sample-source chamber served as the bulb of a helium gas thermometer which was used to measure the temperature during annealing experiments. The rapidly changing temperatures encountered in the warm-up annealing experiments were measured with a lead wire resistance thermometer. Liquid helium could be retained for 16 hours with the alpha-particle source in position and for about 30 hours without the source. The power dissipation of the source approximately accounts for the decreased helium retention time with the source in position.

III. IRRADIATIONS

Experimental measurements of Hall coefficient and resistivity at 4.2°K were made as a function of the integrated alpha-particle flux. In both *n*-type and *p*-type samples these parameters increased monotonically. Following the completion of the irradiation, the samples were held at 4.2°K for as long as 20 hours, and during this time no changes in the electrical properties were observed.

For a degenerate semiconductor, in which the Fermi

level remains deep in the carrier band throughout the irradiation, the probability of occupation of states introduced into the energy gap does not change. Therefore, if the defect production rate is constant, the carrier concentration should change linearly with flux. The reliable calculation of carrier concentration from measured values of Hall coefficient and resistivity is necessary for quantitative interpretation. Some uncertainties exist in such calculations, particularly in the case of *p*-type germanium.¹¹

For an extrinsic semiconductor with carriers in a single energy band, the Hall coefficient may be written as

$$R = \pm r/ne. \quad (1)$$

The proportionality factor, r , for degenerate carriers is equal to unity in the case of a simple energy band with spherical constant energy surfaces in momentum space. For *n*-type germanium the appropriate value is $r=0.79$ due to the multi-ellipsoidal structure of the conduction band. In *p*-type material the holes are distributed in two overlapping bands. The expression for the Hall coefficient for this case has the familiar form

$$R = \frac{r}{p_1 e} \left\{ \left[1 + \frac{p_2}{p_1} \left(\frac{\mu_2}{\mu_1} \right)^2 \right] / \left(1 + \frac{p_2 \mu_2}{p_1 \mu_1} \right)^2 \right\}, \quad (2)$$

where the subscripts 1 and 2 refer to heavy and light holes, respectively. The ratio p_2/p_1 is determined simply by the ratio of effective masses to the $\frac{3}{2}$ power. However, the value of the mobility ratio, μ_2/μ_1 , is uncertain for our case where the carriers are degenerate and the effect of ionized-impurity scattering is important. In view of this uncertainty it is not possible to determine the hole concentration reliably. For the case of lattice scattering, μ_2/μ_1 has been estimated as eight.¹² With this value, the quantity in curly brackets in Eq. (2) is 2.0.

Figure 1 shows results obtained for typical *n*-type and *p*-type samples where the carrier concentrations were computed from Hall coefficient using $r=0.79$ for *n*-type samples and $r=2.0$ for *p*-type samples. In both cases the change of carrier concentration increased linearly with the alpha-particle flux over a considerable range. From the slopes of the curves in Fig. 1, a rate of carrier removal per incident alpha-particle per cm² can be determined and Table I shows the removal rates for three *n*-type and two *p*-type samples which were irradiated at 4.2°K.

The ratio of the maximum carrier removal rate for *n*-type to that for *p*-type germanium is about 2 to 1. Although this result depends on the arbitrary choice of $r=2.0$ for *p*-type samples, it seems that a higher removal rate for *n*-type material is indicated.

The number of lattice displacements created per incident alpha-particle was calculated by the method of

¹¹ B. Abeles and S. Meiboom, Phys. Rev. **95**, 31 (1954).

¹² Willardson, Harman, and Beer, Phys. Rev. **96**, 1512 (1954).

¹⁰ H. Fritzsche, Phys. Rev. **99**, 406 (1955).

TABLE I. Carrier removal rates in alpha-particle-irradiated germanium.

Sample	n_{initial} (carriers/cm ³)	n_{final} (carriers/cm ³)	$-\Delta n/\phi$ (carriers/ α -cm)	$[-\Delta n/\phi]_{\text{Av}}$ (carriers/ α -cm)
Ge(Sb)—No. 2	7.36×10^{17}	4.11×10^{17}	2.75×10^4	2.84×10^4
Ge(Sb)—No. 3	8.02×10^{17}	3.81×10^{17}	2.94×10^4	
Ge(Sb)—No. 5	6.25×10^{17}	3.38×10^{17}	2.84×10^4	
Sample	p_{initial} (carriers/cm ³)	p_{final} (carriers/cm ³)	$-\Delta p/\phi$ (carriers/ α -cm)	$[-\Delta p/\phi]_{\text{Av}}$ (carriers/ α -cm)
Ge(Ga)—No. 2	6.500×10^{18}	5.626×10^{18}	1.30×10^4	1.33×10^4
Ge(Ga)—No. 3	7.012×10^{18}	5.068×10^{18}	1.35×10^4	

Seitz to be 2.79×10^4 defect pairs/ α -cm, when a displacement threshold energy of 30 ev, given by Klontz and Lark-Horovitz,¹³ was used. This value is close to the removal rate of 2.84×10^4 carriers/ α -cm obtained for *n*-type samples. Experiments of various groups have shown that defects in germanium may be produced with energies as low as 14 ev.¹⁴ If this value is used, the calculated number of lattice displacements is 5.94×10^4 defect pairs/ α -cm. Thus for high-energy nucleon irradiations, the value of 30 ev may be an average value which yields good agreement.

The Hall mobility is reduced by the irradiation. Figure 2 shows the variation of Hall mobility with the

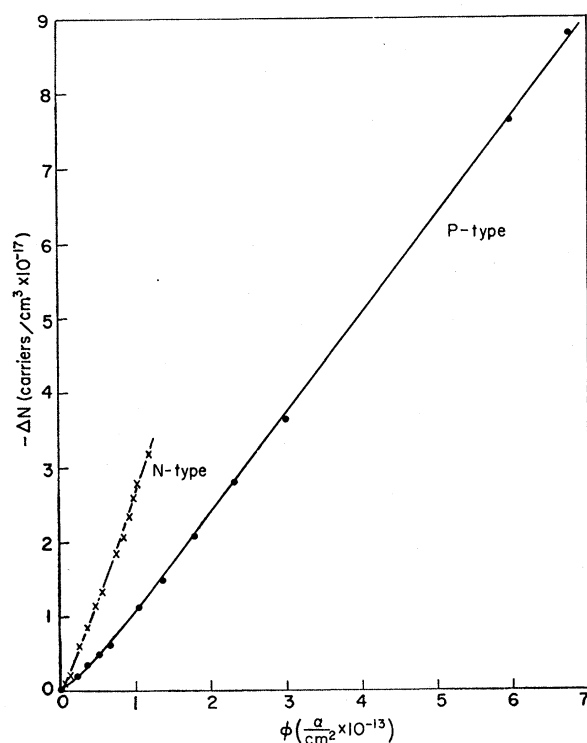


FIG. 1. Change of carrier concentration vs alpha-particle flux. The irradiations and measurements were made at 4.2°K.

¹³ E. E. Klontz and K. Lark-Horovitz, Phys. Rev. **82**, 763 (1951).

¹⁴ J. J. Loferski and P. Rappaport, Phys. Rev. **98**, 1861 (1955).

alpha-particle flux for *n*-type and *p*-type samples. No region is observed in which mobility changes are negligible, so that the estimation of carrier removal rates from resistivity changes alone, neglecting the mobility variation, would be in error. Another important feature of the data is that the mobility in *n*-type samples is very much more sensitive to the flux than is the mobility in *p*-type samples. The change in reciprocal Hall mobility may be taken as a rough estimate of the additional scattering introduced by irradiation. For *n*- and *p*-type samples the ratio is 17.5 per unit flux. The effective mass difference for electrons and holes can hardly explain this large difference if the scattering centers introduced were of the same nature in *n*-type and *p*-type specimens. The stronger *n*-type mobility dependence on flux is probably due to a greater degree of ionization of the defect sites in *n*-type samples.

IV. ANNEALING

In the course of the study of annealing, it was immediately established that appreciable thermal recovery of the irradiation-produced changes in electrical proper-

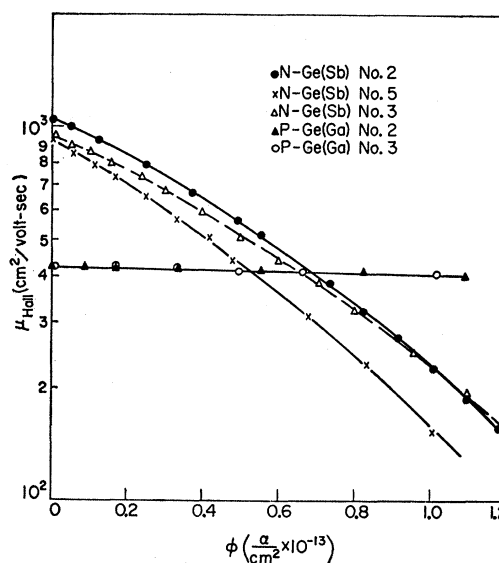


FIG. 2. Hall mobility vs alpha-particle flux.

ties occurred between 4.2°K and 78°K. Three types of annealing experiments were carried out: isothermal, isochronal, and warmup. For isothermal annealing, the sample was maintained at a constant temperature and the changing value of resistivity was measured as a function of time. For isochronal annealing, the electrical properties of the sample were always measured at a reference temperature (4.2°K or 20.4°K). The sample temperature was raised to successively higher values for 20 minutes, with measurements being made between each heat pulse by quenching to the reference temperature. For warmup annealing, the sample temperature was changed continuously, but not uniformly, between 20.4°K and 78°K. The resistivity was measured as a function of both time and instantaneous sample temperature.

All samples, regardless of the type of annealing experiments performed, were eventually raised to a temperature of 78°K and allowed to stand (anneal) there for 10 hours or more. Such a period was found to be long compared to the times in which measurable changes in the electrical properties were detectable. These experiments yield a quantitative comparison of the annealing in *n*-type and *p*-type samples. Table II gives the results of long-time annealing at 78°K for *n*-type and *p*-type samples.

A significant feature is the similarity in the amount of the thermal recovery observed in *n*-type and *p*-type samples. This means that the annealing removes acceptors and donors in the same proportion that they were produced by the irradiation. Since a preferential annealing of defects associated with either acceptors or donors would be manifested by a significant difference in the recovery of *p*-type and *n*-type samples, this result indicates that such selective annealing does not occur.

Similarities were also found in other features of the annealing experiments. The result of an isochronal annealing experiment is shown in Fig. 3, where the recovery behavior of a *p*-type sample is shown. The resistivity measured at a reference temperature following 20-minute heat pulses is plotted as a function of the annealing temperature. As indicated in Fig. 3, thermal recovery is not detected for annealing temperatures as high as 22°K. In order to further substantiate this result, long-time isothermal annealing was performed at 20.4°K, the normal boiling point of liquid hydrogen.

TABLE II. Comparison of 78°K annealing of *n*-type and *p*-type samples. All samples were irradiated at 4.2°K, then annealed for 10 hours or more at 78°K. Measurements were made at 4.2°K.

	Sample	$\Delta n_{\phi} _{total}$ (carriers/cm ³)	Δn_{anneal} (carriers/cm ³)	$\Delta n_A / \Delta n_{\phi}$ (%)	Average ratio (%)
<i>n</i> type	Ge(Sb)—No. 2	3.25×10^{17}	8.8×10^{16}	27	25
	Ge(Sb)—No. 3	4.21×10^{17}	10.4×10^{16}	25	
	Ge(Sb)—No. 5	2.87×10^{17}	5.7×10^{16}	24	
<i>p</i> type	Ge(Ga)—No. 2	8.72×10^{17}	2.0×10^{17}	23	22
	Ge(Ga)—No. 3	19.44×10^{17}	4.12×10^{17}	21	

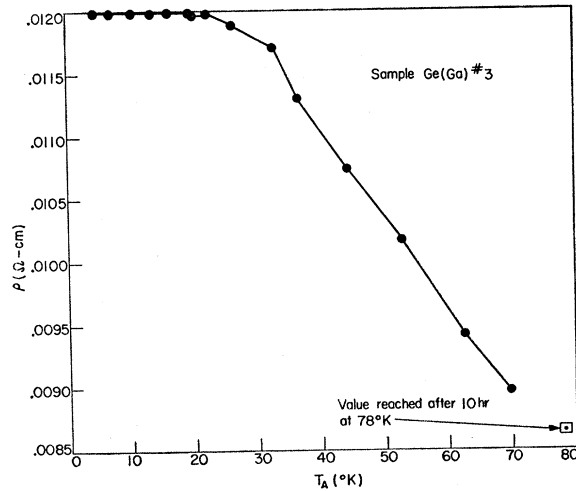


FIG. 3. Isochronal anneal vs temperature of anneal. The measurements were made at 4.2°K after 20-minute heating periods.

No measurable change in resistivity was observed during the 14 hours that the sample remained at 20.4°K. Thus, it was permissible to use 20.4°K as the reference point for annealing temperatures between 20.4°K and 78°K, a result which greatly facilitated the ease and accuracy of the experiments in this region. Thermal recovery was experimentally detected after a 20-minute anneal at 26°K and the recovery proceeded more rapidly at higher temperatures. The annealing behavior of the *n*-type sample followed this same pattern.

The similarity in the annealing processes for *n*-type and *p*-type specimens is further confirmed by the warmup annealing experiments carried out with both types of samples. The sample temperature varied smoothly, although not uniformly, from 20.4°K to

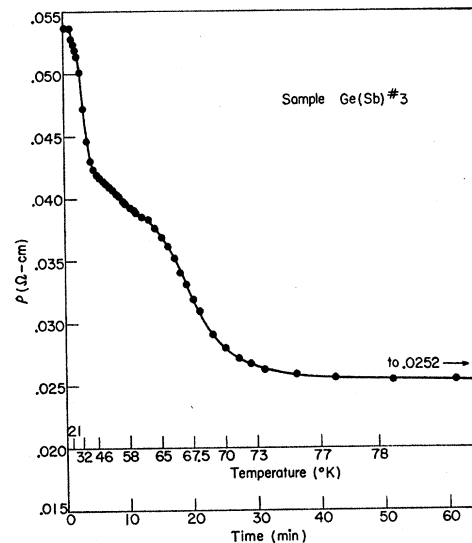


FIG. 4. Resistivity of irradiated germanium during warmup to 78°K.

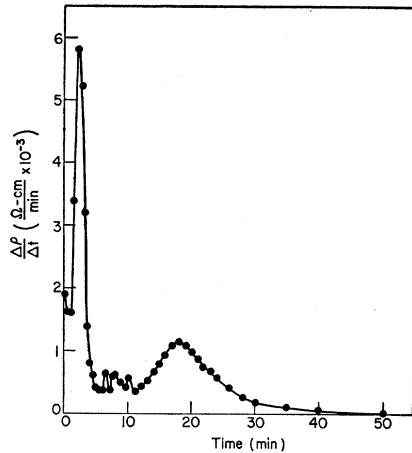


FIG. 5. Plot of $d\rho/dt$ vs time during warmup anneal of n -type germanium. $T=20.4^\circ\text{K}$ at $t=0$.

78°K after the coolant (liquid hydrogen) was allowed to evaporate from the inner Dewar. Figure 4 shows the results of such an experiment on an n -type sample. Two distinct regions of thermal recovery can be distinguished, one with the maximum recovery rate near 33°K and the second with the maximum recovery rate near 66°K . The two distinct regions of annealing are more strikingly exposed in Fig. 5, where the time rate of change of the resistivity ($d\rho/dt \approx \Delta\rho/\Delta t$) is plotted as a function of the instantaneous sample temperature. A similar curve was obtained for a p -type sample. The irradiation induced changes were not large in the p -type case and consequently the accuracy of the data was not so good as for the n -type sample. The two annealing stages can however definitely be identified.

The warmup curve of Fig. 4 suggests that two separate and distinct processes are active in the annealing which occurs between 4.2°K and 78°K . Establishing whether or not the two annealing regions are completely separable and thus allowing each to be considered independently, is important for the interpretation of the experimental data. Isothermal annealing at appropriate temperatures was employed to establish this point and to determine the order of the kinetic reaction for the lower temperature recovery process.

Figure 6 shows the results of isothermal annealing of an n -type sample at 26°K , 33°K , and 50°K , the latter temperature being midway between the two suspected annealing temperature regions. The small, sharply curved region of the 26°K curve of Fig. 6 was caused by temperature instability in the first two minutes of this anneal. The data clearly indicate that the two regions of thermal recovery are independent and separable, as evidenced by the absence of additional thermal recovery at 50°K following the completed isothermal anneal at 33°K . The asymptotic value reached by the resistivity in annealing at 33°K as compared to the value reached

by annealing at 78°K reveals that 45% of the total annealing occurs in the lower temperature process.

V. DETERMINATION OF ANNEALING ACTIVATION ENERGY

The theory of kinetic rate processes has been applied with considerable success to the description and interpretation of the thermal recovery of irradiation effects in solids. The theory has been formalized recently by Primak,¹⁵ who considered processes with unique activation energies and with a distribution of activation energies. Consider an annealing process which proceeds according to the relation

$$-dN/dt = cN^n, \quad 0 \leq N \leq N_0, \quad (3)$$

where N is the defect concentration at time, t , during an intermediate stage of the annealing, c is a temperature-dependent coefficient, n is the order of the reaction (not restricted to integer values), and N_0 is the concentration of defects immediately after irradiation which are annihilated or otherwise undergo a reaction during the annealing process being considered.

In this work the measured sample parameter was the electrical resistivity, ρ , because of experimental limitations which precluded the reliable measurement of the Hall effect during the course of the annealing experiments. The problem which now arises is to determine a method of relating the experimental data on resistivity changes to the quantity of physical interest, the defect concentration changes.

In metals, the irradiation-induced changes in the residual resistivity can be assumed to be proportional to the irradiation-produced defect concentration. This

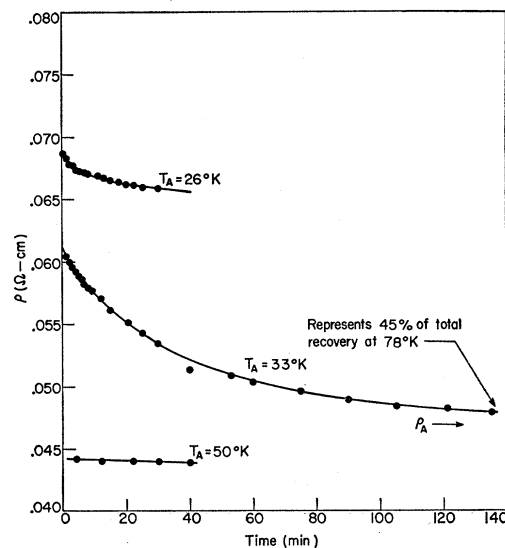


FIG. 6. Isothermal annealing of alpha-particle-irradiated n -type germanium.

¹⁵ W. Primak, Phys. Rev. **100**, 1677 (1955).

assumption is based on the observation¹⁶ that the residual electrical resistivity of a metal increases linearly with increasing impurity concentration. Therefore the interpretation of the data is quite straightforward in such cases.

In semiconductors the changes of resistivity due to irradiation arise from changes both in carrier concentration and in mobility, and therefore the evaluation of the data is not so straightforward as in the case of metals. The problem of physical interpretation of the data reduces to the determination of the behavior expected for resistivity changes when the defect concentration changes obey a kinetic rate equation as given by Eq. (3).

The effect of the changing mobility and carrier concentration on the interpretation of annealing-caused resistivity changes is investigated in Appendix I, using a method suggested by Fan. For the small values of $\Delta\rho/\rho$ encountered in these experiments, a defect concentration variation which obeys Eq. (3) will, to a good approximation, result in a resistivity variation given by

$$-d\rho/dt = h(\rho - \rho_A)^n, \quad (4)$$

where h is a constant, ρ_A is the asymptotic value of resistivity, reached after completion of the annealing process being considered, and n is the order of the reaction. Resistivity variations will thus be interpreted on the basis of this equation, which will be considered equivalent to Eq. (3). For the case in which n is unity, a plot of $\log(\rho - \rho_A)$ vs time for isothermal annealing will give a straight line. For other values of n , a plot of $\log(\rho - \rho_A)$ vs $\log(\text{time})$ will yield a straight line of slope $1/(1-n)$.

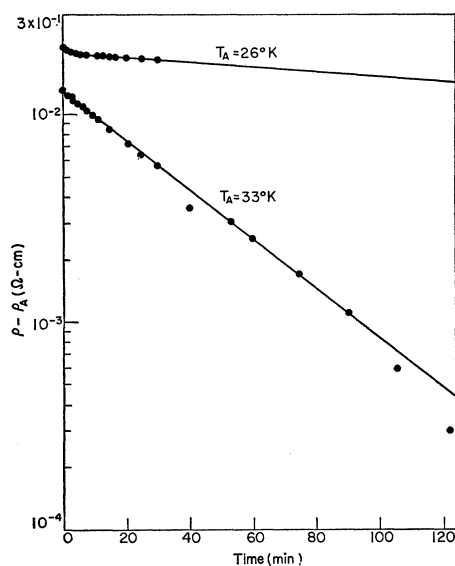


FIG. 7. Semilogarithmic plot of $(\rho - \rho_A)$ vs time for data of Fig. 6.

¹⁶ J. O. Linde, *Elektrische Widerstandseigenschaften der Verdünnten Legierungen des Kupfers, Silbers und Goldes* (Haken Ohlssons Buchdruckerei, Lund, 1939).

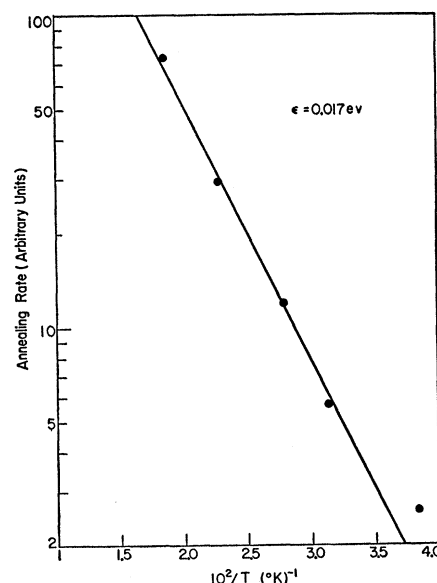


FIG. 8. Semilogarithmic plot of annealing rate vs $10^2/T$ for isochronal annealing data.

Figure 7 shows a plot of $\log(\rho - \rho_A)$ vs time for the isothermal annealing data of Fig. 6. The data indicate that the proper value for n is unity. Thus Eq. (4) becomes

$$-d\rho/dt = h(\rho - \rho_A). \quad (5)$$

It is generally assumed that the temperature dependence of the rate constant, h , is given by the usual exponential dependence involving an activation energy,

$$h = A e^{-\epsilon/kT}, \quad (6)$$

where ϵ is the thermal activation energy and A is a constant.

For isothermal annealing at two different temperatures, T_1 and T_2 , the activation energy can be determined from Eq. (5) and Eq. (6). For the data of Fig. 7, the value so obtained is

$$\epsilon = 0.018 \text{ ev.}$$

Isochronal annealing may be considered as short-duration isothermal annealing at various temperatures. Since the total resistivity change which occurs upon the completion of the given kinetic process has been determined, the data may be analyzed from Eq. (5) and Eq. (6). From Eq. (5) a plot of $\ln h$ as a function of $1/T$ gives a straight line with a slope of $-\epsilon/k$. Such a plot is shown in Fig. 8, the value obtained for the activation energy being

$$\epsilon = 0.017 \text{ ev,}$$

which is in good agreement with the value obtained from isothermal annealing.

If Eq. (5) is assumed to describe the low-temperature annealing rigorously, then it is possible to compare

rates of change expected at various temperatures. By using the above value of ϵ (0.017 eV) and comparing the known rates at 33°K to the expected rate at 20.4°K, it is found that a measurable change in resistivity (about 2½%) is predicted for the 14-hour period that the sample remained at 20.4°K. As pointed out earlier, no such change was observed. The conclusion is that the annealing data are qualitatively well described by the use of such an equation but that quantitatively complications can arise, in the interpretation of what must be complicated phenomena on the basis of such a simple theory.

The warmup curves can be analyzed easily because of the near temperature independence of resistivity of the samples. For such samples, the value of h is determined directly from the plots of Fig. 5 and Fig. 6 by finding corresponding values of $d\rho/dt$ and $(\rho - \rho_A)$ for a given temperature. The activation energy may then be easily obtained, the value for the low-temperature process being

$$\epsilon \cong 0.014 \text{ eV.}$$

Since the annealing changes are so rapid in this temperature region, this value must be regarded only as approximate. Thus it is concluded that this low-temperature process follows a first-order kinetic rate equation with a unique thermal activation energy of about 0.02 eV.

Analysis of the warm-up curves does not yield a unique value for the activation energy when applied to the higher temperature recovery. The value obtained was in the region of 0.1 eV to 0.2 eV. The data in this temperature region are, however, insufficient for a complete analysis.

This low-temperature annealing might be attributed to the recombination of interstitials with certain types of nearby vacant lattice sites at temperatures too low to permit appreciable interstitial diffusion through the lattice. Such a configuration of vacancies and interstitials would be less probable and hence fewer in number than interstitials displaced some distance from the vacancy. This would then explain the small fraction (10%) of the irradiation-produced damage which anneals in this process. The explanation of the annealing as mutual annihilation of vacancies and interstitials is further supported by the fact that the annealing is the same in n -type and p -type samples. If either vacancies or interstitials were selectively annihilated or if clustering of one of the defects occurred, then the annealing should produce distinctly different effects in n -type and p -type samples rather than the observed symmetrical behavior.

APPENDIX

The electrical resistivity is written as

$$\rho = 1/(ne\mu), \quad (7)$$

where n is the carrier concentration, e is the electronic charge, and μ is the carrier mobility.

Immediately following the irradiation ($t=0$) the concentration of annealable defects is N_0 . The initial state of the semiconductor is described by a resistivity ρ_0 , carrier concentration n_0 , and mobility μ_0 , where

$$\rho_0 = 1/(n_0e\mu_0). \quad (8)$$

After completion of the annealing process ($t=\infty$), the annealable defect concentration has been reduced to zero and the final state of the semiconductor is described by an asymptotic value of resistivity ρ_A , carrier concentration n_A , and mobility μ_A , where

$$\rho_A = 1/(n_Ae\mu_A). \quad (9)$$

Assuming a direct proportionality between changes in carrier concentration and changes in defect concentration ($n_A - n = b'N$) yields

$$n = n_A - (bN/N_0), \quad b = n_A - n_0. \quad (10)$$

It is logical to assume a direct proportionality between changes in the reciprocal of mobility and changes in defect concentration ($1/\mu - 1/\mu_A = c'N$), which yields

$$\frac{1}{\mu} = \frac{1}{\mu_A} + \frac{cN}{N_0}, \quad c = \frac{1}{\mu_0} - \frac{1}{\mu_A}. \quad (11)$$

Using Eqs. (7), (10), and (11), one obtains

$$N = \frac{en_A N_0}{c + eb\rho} (\rho - \rho_A), \quad (12)$$

$$\rho_0 \geq \rho \geq \rho_A, \quad N_0 \geq N \geq 0,$$

and

$$\frac{dN}{dt} = \frac{en_A N_0}{(c + eb\rho)^2} (c + eb\rho_A) \frac{d\rho}{dt}. \quad (13)$$

Substituting Eqs. (12) and (13) into Eq. (1) yields

$$\frac{-d\rho}{dt} = \frac{aen_A N_0}{c + eb\rho_A} \left[\frac{c + eb\rho}{en_A N_0} \right]^{2-n} (\rho - \rho_A)^n. \quad (14)$$

Therefore, if changes in $(c + eb\rho)^{2-n}$ caused by annealing are small, i.e., if $[(c + eb\rho)/en_A N_0]^{2-n}$ is almost a constant, then Eq. (14) may be considered as being the same type as Eq. (3) and the resistivity data can be analyzed on the basis of a kinetic rate equation. Since $c + eb\rho$ is a linear function of ρ , its variation may be established by evaluation at the extrema of the variable ($\rho = \rho_0$ and $\rho = \rho_A$).

For the annealing experiments under consideration,

$c+ebp$ varies by about $\pm 3\%$ from its average value over the complete experimental range. For small values of the reaction order, n , it can be stated that for experiments considered in this work, a defect concentration reaction of the type of Eq. (3) will result in a variation of resistivity which obeys Eq. (4).

ACKNOWLEDGMENTS

The author wishes to express his appreciation for the encouragement and guidance of the late Dr. K. Lark-Horovitz throughout the course of this work. He is also indebted to Dr. H. Y. Fan for valuable comments and suggestions.

Theory of the Hall Effect in Ferromagnetic Substances

J. M. LUTTINGER*

École Normale Supérieure, Laboratoire de Physique, Paris, France

(Received July 2, 1958)

The Hall effect in ferromagnetic substances is computed on the basis of a simple model, making use of the transport theory of Kohn and Luttinger. The calculation is rigorous, but assumes a slowly varying scattering potential, a simple band, and very few conduction electrons. None of these assumptions are very realistic for a true ferromagnet, but we are interested here in only giving a discussion of the types of contributions which can occur. Terms related to those previously found by Smit and by Karplus and Luttinger, and some new ones, are found. In addition, some comments of Smit on the general problem of the ferromagnetic Hall effect are discussed.

1. INTRODUCTION

IN recent years there has been considerable discussion of the anomalous Hall effect in ferromagnetic substances, from several points of view. All serious attempts to explain this phenomenon have used as a basic model magnetically polarized electrons moving under the influence of an external field, and have attributed its origin to the presence of spin-orbit coupling. The difference has been in the effect of the spin-orbit coupling considered. Karplus and Luttinger looked for contributions which arise from a modification of the acceleration effects due to the electric field, and from off-diagonal parts of the density matrix. Smit, on the other hand, considered the modification which occurs in the scattering processes within the framework of conventional transport theory. Both of these theories give results which are not in contradiction with experiment, though neither of them fits all the data. On the other hand, some of the conclusions of the theory of Karplus and Luttinger have been seriously questioned by Smit, so that the entire subject has recently been shrouded in a thick fog.

For this reason, we thought it worth while to consider the subject anew, from a somewhat different point of view. There exists a model (for impurity-limited resistivity) in which the entire transport theory can be put on a rigorous and systematic basis. This is the theory of Kohn and Luttinger,¹ which develops the

stationary-state density matrix of the system in powers of the strength of the scattering potential. Using this model, we have calculated the entire anomalous Hall effect. Terms of the Smit type, the Karplus-Luttinger type, and some others, all appear automatically in this treatment. Although the model itself is not very realistic, and the further simplification necessary to complete the calculation makes it even less so, we still believe it is of some interest in showing the types of contributions which can occur.

The paper is organized as follows. In Sec. 2 the theory of KLI is summarized and reduced to a usable form without any further approximations. In Sec. 3, the contribution of the spin-orbit coupling (which gives rise to the Hall current) is separated out. In Sec. 4 the equations are solved, and the Hall current is calculated rigorously in the effective-mass limit. In Sec. 5 we discuss the results and compare them with the previous ones. Finally, in Appendix A, some of the criticisms of Smit are considered within the framework of the present theory.

2. GENERAL THEORY

In this section we shall develop the general formulas which enable us to calculate the contribution of spin-orbit coupling to the Hall effect. From KLI, we can expand that part of the density matrix which is linear in the external field (f), in ascending powers of λ (which is some dimensionless measure of the strength of the scattering potential). The leading term in f is of order λ^{-2} , and to this order conventional transport theory holds. The new features of KLI (corrections to transport equation, contributions from off-diagonal ele-

* Permanent address: Department of Physics, University of Pennsylvania, Philadelphia 4, Pennsylvania.

¹ W. Kohn and J. M. Luttinger, Phys. Rev. **108**, 590 (1957). We shall refer to this paper as KLI in what follows. As in KLI, we shall not indicate explicitly here the vector character of k or r . Thus $e^{ik \cdot r}$ means $e^{i\mathbf{k} \cdot \mathbf{r}}$ and $k \neq k'$ means $\mathbf{k} \neq \mathbf{k}'$ throughout.